

---

# APPROXIMATIVE POLICY ITERATION FOR EXIT TIME FEEDBACK CONTROL PROBLEMS DRIVEN BY STOCHASTIC DIFFERENTIAL EQUATIONS USING TENSOR TRAIN FORMAT

---

A PREPRINT

**Konstantin Fackeldey**  
Technische Universität Berlin  
Strasse des 17. Juni 135  
10623 Berlin, Germany  
fackeldey@math.tu-berlin.de

**Mathias Oster**  
Technische Universität Berlin  
Strasse des 17. Juni 135  
10623 Berlin, Germany  
oster@math.tu-berlin.de

**Leon Sallandt**  
Technische Universität Berlin  
Strasse des 17. Juni 135  
10623 Berlin, Germany  
sallandt@math.tu-berlin.de

**Reinhold Schneider**  
Technische Universität Berlin  
Strasse des 17. Juni 135  
10623 Berlin, Germany  
schneider@math.tu-berlin.de

October 12, 2020

## Abstract

We consider a stochastic optimal exit time feedback control problem. The Bellman equation is solved approximatively via the Policy Iteration algorithm on a polynomial ansatz space by a sequence of linear equations. As high degree multi-polynomials are needed, the corresponding equations suffer from the curse of dimensionality even in moderate dimensions. We employ tensor-train methods to account for this problem. The approximation process within the Policy Iteration is done via a Least-Squares ansatz and the integration is done via Monte-Carlo methods. Numerical evidences are given for the (multi dimensional) double well potential and a three-hole potential.

## 1 Introduction

Optimal control of ordinary differential equations (ODE) is a field of mathematics and engineering, where we minimize a cost functional constrained by a controlled ODE. Substituting the ODE by a stochastic differential equation (SDE) we obtain a stochastic optimal control problem. The inherent structure of the cost functional determines the behavior of the optimization problem. Within this context several formulations have been investigated. Among them are finite and infinite horizon problems and exit time problems. For the latter, one determines the optimal control to reach a predefined exit set with respect to the cost functional. An inherent difficulty is that the stopping time is not known in advance and depends not only on the control but also on the stochastic process.

Optimal control problems of stochastic processes have been utilized in various fields of applications, such as finance, engineering or molecular dynamics, see e.g.[1–3]. Subsequent to the latter in [4, 5] this optimal control setting has been applied to the characterization of free energy of an uncontrolled dynamical system. Different numerical methods have been developed and are now widely used and further investigated, see

e.g. [6–10]. A popular approach is approximating the value function by solving either the Bellman or the Hamilton-Jacobi-Bellman (HJB) equation.

For low dimensions  $n \leq 3$  the HJB equations, corresponding to deterministic and stochastic optimal control problems, have been treated by Finite Element [11] and Finite Difference methods [12, 13], including Semi-Lagrangian methods [14–17]. These methods are based on grids and are facing the curse of dimensions, which prevents the treatment of large spatial dimensions  $n$ . Popular approaches to get rid of the curse of dimensions are sparse grids [18, 19], Tensor trains combined with Galerkin [20] or minimal residual [21] methods, or using Max-Plus algebra [22], see also [23–25] for further ideas. Nowadays deep neural networks (DNN) have become an attractive tool for solving the HJB [26–28]. In our approach we address the high-dimensionality by using Monte-Carlo integration and Tensor Train (TT) formats and the non-linearity by using the Policy Iteration algorithm [29–31].

Here, we consider some stochastic process  $X_t$  starting in  $X_0 = x$  on a potential landscape (cp Fig 1). Our goal is to modify  $X_t$  by a control  $u_t$  such that the process exits a predefined set  $\Xi$ . Of course, there are many possible controls, driving the system out of  $\Xi$ . Our goal is it to find the optimal control with respect to a certain cost function  $\mathcal{J} = \mathcal{J}(x, u)$ .

It is worth mentioning, that the infinitesimal version of the Bellman equation is the Hamilton-Jacobi-Bellman (HJB) equation. If the structure of the stochastic part is modeled by a Wiener process, it appears within the HJB as a Laplace operator [32–35]. Solving the HJB could be realized by adapting the method in [20], where the deterministic HJB has been approximated by using Tensor Trains. Note that other function approximators like Neural Networks can be used for our algorithm. Indeed, in the HJB case, the Policy Iteration algorithm leads to solving backward Kolomogorov equations, which have previously been treated with neural networks in [36].

In the following section we introduce the optimal control problem and the concept of the Bellman equation. Section 3 is devoted to the Policy Iteration in a function space. In the subsequent sections the Least-Squares approximation and our function approximator, the Tensor Trains, are introduced. The final section is devoted to the presentation of the numerical results, where we cover some low-dimensional problems and one problem in dimension six.

## 2 Exit Time Control Problem of a Stochastic ODE

We assume, that the stochastic ODE in  $\Xi \subset \mathbb{R}^n$  open, given by

$$\begin{aligned} dX_t &= b(X_t)dt + \sigma(X_t)dW_t + g(X_t)u_t dt \\ X_0 &= x, \end{aligned} \tag{1}$$

describes the state of a system at time  $t$ , where  $X_t \in \mathbb{R}^n$ ,  $b : \mathbb{R}^n \rightarrow \mathbb{R}^n$  is the gradient of a smooth potential  $U$  with bounded derivatives,  $g : \Xi \rightarrow \mathbb{R}^{n,m}$ ,  $\sigma : \mathbb{R}^n \rightarrow \mathbb{R}^{n,n}$  are smooth with bounded derivatives and  $W$  is a Wiener process. Additionally,  $u_t \in \mathbb{R}^m$  is a control parameter adapted to the process  $X_t$ . In the context of dynamic programming  $u_t$  is also known as action, decision or policy of the controller. For each control  $u$  we can define the exit time  $\eta$

$$\eta = \inf\{t > 0 | X_t \notin \Xi\}$$

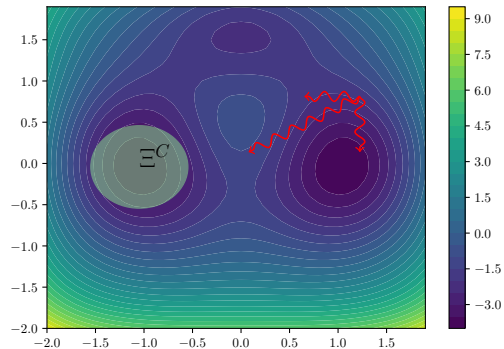


**Figure 1:** At a given point on the right hand side different trajectories of the stochastic process are visualized by the red arrows. We now seek for the optimal control driving the process out of the set  $\Xi$ .

and the cost function

$$\mathcal{J}(x, u) = \mathbb{E} \left[ \int_0^\eta c(X_t) + u_t^T B u_t dt | X_0 = x \right],$$

where  $c : \mathbb{R}^n \rightarrow \mathbb{R}$  is some given continuous, positive function and  $B \in \mathbb{R}^{m,m}$  is positive definite.

Our goal is it to find the control  $u$  with minimal cost, i.e.

$$\min_u \mathcal{J}(x, u).$$

Here, we do not specify the space that we minimize over. Formally speaking, we consider the space of controls mapping to  $\mathbb{R}^m$  that are measurable and adapted to a filtration induced by the Brownian motion. As we are later considering feedback controls, we omit the technical details and instead refer to [37, 38] and references therein.

We define the value function  $v^* : \mathbb{R}^n \rightarrow \mathbb{R}$  as minimum of the cost functional over all controls, i.e.

$$v^*(x) := \min_u \mathcal{J}(x, u) \text{ for all } x \in \Omega.$$

The control  $u^*$  is optimal if  $v^*(x) = \mathcal{J}(x, u^*)$  holds.

Under the assumption that there exists a Lipschitz continuous feedback control  $\alpha : \mathbb{R}^n \rightarrow \mathbb{R}^m$  with finite cost for any initial state  $x \in \Omega$  we replace (1) by the closed loop system

$$dX_t = b(X_t) + \sigma(X_t) dW_t + g(X_t) \alpha(X_t) \quad (2)$$

and denote the corresponding state by  $X_t^\alpha$  to stress the dependence on the feedback. It has been shown under suitable regularity assumptions on the right hand side of the SDE, that (2) is well defined and is differentiable with respect to the initial values [39, chapter 2],[40]. Since we are considering time-homogeneous Itô diffusions, our processes fulfill the (strong) Markov property [41].

In the following we only consider feedback laws that give us finite costs. Thus, we define the policy evaluation function  $v^\alpha$  with respect to a fixed feedback law  $\alpha$  as

$$v^\alpha(x) := \mathbb{E} \left[ \int_0^\eta c(X_t^\alpha) + \alpha(X_t^\alpha)^T B \alpha(X_t^\alpha) dt | X_0 = x \right]. \quad (3)$$

**Remark 1.** In our algorithm we will later compute  $v^\alpha$  approximately. In this case the equality (3) is not given and we distinguish between the policy evaluation function, which is  $v^\alpha$  as in (3) and the policy estimation function, which is  $v^\alpha$  computed by our algorithm.

We define the set of feedback laws that induce finite costs

$$F = \{ \alpha : \mathbb{R}^n \rightarrow \mathbb{R}^m \mid v^\alpha(x) < \infty \text{ for all } x \in \mathbb{R}^n \}$$

and assume that there exists an optimal, Lipschitz continuous feedback law. This ensures that the value function is the policy evaluation functional of the optimal feedback, i.e.

$$v^* = v^{\alpha^*}.$$

If the value function  $v^*$  is known and differentiable, the optimal control is given explicitly by [42]

$$\alpha^*(x) = -\frac{1}{2} B^{-1} g(x)^T \nabla v^*(x).$$

Moreover, abbreviating  $r^\alpha(x) = c(x) + \alpha(x)^T B \alpha(x)$  and  $\tau \wedge \eta = \min\{\tau, \eta\}$ , a stochastic Bellman equation [43] is obeyed for every  $\tau > 0$

$$v^*(x) = \mathbb{E} \left[ \int_0^{\tau \wedge \eta} r(X_t^{\alpha^*}) dt + v^*(X_{\tau \wedge \eta}^{\alpha^*}) | X_0 = x \right] \quad (4)$$

$$\alpha^*(x) = -\frac{1}{2} B^{-1} g(x)^T \nabla v^*(x) \quad (5)$$

with Dirichlet boundary condition

$$v^*(x) = 0 \text{ on } \partial\Xi.$$

We later employ the Policy Iteration algorithm to solve this coupled equation by alternating between the value updates given by (4) and the policy updates given by (5). In preparation to that we first notice that by fixing a policy  $\alpha$  this coupled equation becomes uncoupled and a linear function equation is remaining

$$v^\alpha(x) = \mathbb{E} \left[ \int_0^{\eta \wedge \tau} r(X_t^\alpha) dt + v^\alpha(X_{\eta \wedge \tau}^\alpha) \right] := \mathbb{E} \left[ \int_0^{\eta \wedge \tau} r(X_t^\alpha) dt + v^\alpha(X_{\eta \wedge \tau}^\alpha) | X_0^\alpha = x \right]. \quad (6)$$

Note, that the expectation value is a conditional expectation value with respect to the initial value  $X_0 = x$ . For the ease of notation, in the sequel we sometimes drop the condition  $X_0 = x$  when the context is clear.

### 3 Policy Iteration

A typical approach to solve the Bellman equation (6) would be to use a fixed point iteration in the values, with some given initial guess. This method is known as value iteration e.g. [44, Chapter 3]. When computing (6) with the value iteration, a sequence of functions  $\{v_k\}_k$  is generated, such that  $v_k \rightarrow v^*$  under suitable conditions. However, for a value iteration it must be clarified how to discretize the policy(space).

In the following, we take a different path by using the Policy Iteration, where a sequence of policies  $\{\alpha_k\}_k$  instead of values is generated. It has been understood in [21] that the policy evaluation function  $v^\alpha$  in the deterministic setting can be computed via the Koopman operator [45]. The Koopman operator is a linear transfer operator allowing to transfer a system with a non-linear evolution to a linear system in function space. The structure of the eigenvalues and eigenfunctions of the Koopman operator have been investigated to obtain a coarse grained description of the system [46–49].

To do so we rewrite (6) by using the Koopman operator [50–53] with a slight modification to incorporate the exit time

$$K_\tau^\alpha[v] = \mathbb{E}[v(X_{\eta \wedge \tau}^\alpha) | X_0^\alpha = x].$$

This allows us, to reformulate equation (6) as operator equation

$$(I - K_\tau^\alpha)v(x) = \mathbb{E} \left[ \int_0^{\eta \wedge \tau} r(X_t^\alpha) dt | X_0^\alpha = x \right]. \quad (7)$$

With the operator equation (7) we can now give the Policy Iteration algorithm.

---

**Algorithm 1:** Policy Iteration for solving (4)

---

**input** : A Policy  $\alpha_0 \in F$ .

**output** : An approximation of  $v^*$  and  $\alpha^*$ .

Set  $k = 0$ .

**while** *not converged* **do**

    Solve the linear equation

$$(I - K_\tau^{\alpha_k})v_k(x) = \mathbb{E} \left[ \int_0^{\eta \wedge \tau} r(X_s^{\alpha_k}) ds | X_0^\alpha = x \right], \quad (8)$$

    then update the policy according to

$$\alpha_{k+1}(x) = -\frac{1}{2} B^{-1} g(x)^T \nabla v_k(x).$$

$k = k + 1$ .

**end**

---

Note that in the algorithm we have to choose an initial policy  $\alpha_0 \in F$ . In some cases this is a particular hard challenge, as the policy has to lead to finite cost for every initial state  $x$ . However, the Wiener process ensures that the uncontrolled dynamics driven by a potential arrive at the exit set in finite time almost surely. Thus, we initialize the Policy Iteration with the zero control  $\alpha \equiv 0$ . For solving (8) in the above algorithms we face the following two problems:

**Linearized Bellman** In principle the point values of the linearized Bellmann equation (8) can be computed by Monte Carlo Methods such as Euler-Mayurama. Let us assume that we have computed pointwise values. How can we 'interpolate' between these values to obtain an approximation of the policy evaluation function? For this purpose we propose a Least Squares approach, where the nodes are sampled randomly, i.e. we use Monte Carlo integration. We call this approach *variational Monte Carlo*, introduced in section 4.

**Model Class** The equation (8) is given in an infinite dimensional space  $V$  and we need a finite dimensional ansatz space, or at least a set  $U \subset V$  of computable approximation  $v_{\varepsilon,k}$  of  $v_k$  to achieve a desired accuracy  $\varepsilon$ . We choose the intersection of a scaled ball with a submanifold  $\mathcal{M}$ . Therefore, we have to approximate the function  $v_k \in U \subset \mathcal{M} \subset V$ . We propose Tensor Trains and Tree based Tensors for  $\mathcal{M}$  in Section 5 to tackle this challenge.

## 4 Variational Monte-Carlo

We now elaborate on how to tackle the computational bottleneck, i.e. the linearized Bellman equation (8),

$$\begin{aligned} (I - K_\tau^\alpha)v_k(x) &= \mathbb{E}\left[\int_0^{\eta \wedge \tau} r(X_s^{\alpha_k})ds | X_0^\alpha = x\right]. \\ \iff v_k(x) &= \mathbb{E}\left[\int_0^{\eta \wedge \tau} r(X_s^{\alpha_k})ds + v_k(X_{\eta \wedge \tau}^\alpha) | X_0^\alpha = x\right]. \end{aligned} \quad (9)$$

This is done in three major steps. First, we interpret the above equation as a fixed-point equation, then we formulate the subproblems as a Least Squares problem on a finite dimensional function space and, finally, we use Monte-Carlo quadrature to integrate within the state and probability space.

The policy  $\alpha := \alpha_k$  is given and we assume that  $\hat{v}$  on the r.h.s. of the equation below is given as well. Let us introduce  $\tilde{v} \in V$  such that

$$\tilde{v}(x) := \mathbb{E}\left[\int_0^{\eta \wedge \tau} r(X_s^\alpha)ds + \hat{v}(X_{\eta \wedge \tau}^\alpha) | X_0^\alpha = x\right], \quad x \in \Omega,$$

Note that if  $\tilde{v} = \hat{v}$  we have found a solution to (9). As this equation is posed in an infinite dimensional function space, we first rewrite it as a Least-Squares problem on a finite dimensional subspace.

More exactly, consider the Hilbert space  $V := L^2(\Omega)$ , (or more generally  $V := L_2(\Omega, \rho)$  with some probability density  $\rho$ ) such that  $\hat{v}, \tilde{v} \in V$ . Then, we have

$$\tilde{v} = \arg \min_{v \in V} \mathcal{R}^\alpha(v, \hat{v}), \quad \mathcal{R}^\alpha(v, \hat{v}) = \|v(\cdot) - \mathbb{E}\left[\int_0^{\eta \wedge \tau} r(X_s^\alpha)ds + \hat{v}(X_{\eta \wedge \tau}^\alpha) | X_0^\alpha = \cdot\right]\|_V^2$$

and since  $\tilde{v} \in V$ , we have  $\mathcal{R}^\alpha(\tilde{v}, \hat{v}) = 0$ . Indeed, we are seeking a solution  $\hat{v} = \tilde{v}$  which constitutes a fixed point problem

$$\tilde{v} = \arg \min_{v \in V} \mathcal{R}^\alpha(v, \tilde{v}), \quad \mathcal{R}^\alpha(v, \tilde{v}) = \|v - \mathbb{E}\left[\int_0^{\eta \wedge \tau} r(X_s^\alpha)ds + \tilde{v}(X_{\eta \wedge \tau}^\alpha) | X_0^\alpha = \cdot\right]\|_V^2. \quad (10)$$

However, finding the exact minimizer  $\tilde{v} \in V$  is infeasible, and thus we further restrict to a finitely representable compact subset  $U \subset V$ .

Classically,  $U \subset V$  is a closed ball of some finite dimensional subspace  $V_p \subset V$ . However, in many applications the subspace  $V_p$  is high-dimensional, which makes computations impracticable. Thus, we introduce a lower dimensional submanifold  $\mathcal{M} \subset V_p$  and consider  $U \subset \mathcal{M} \subset V_p$  to be a compact subset feasible for computational treatment, having an intrinsic data complexity, which can be handled by our technical equipment. In our case  $\mathcal{M}$  is the set of tensor trains of bounded (multi-linear) rank  $\mathbf{r} = (r_1, \dots, r_n)$  and  $U$  is the set of rank  $\mathbf{r}$  tensors with uniformly bounded norm embedded in the space  $\mathcal{M} \subset V_p$  of tensor product polynomials of multi-degree  $\mathbf{p}$ , which will be covered in detail in the following section. For  $U \subset \mathcal{M}$  the Least-squares approximation is defined by the minimizer (10)

$$v_U^\alpha = \arg \min_{v \in U} \mathcal{R}^\alpha(v, v). \quad (11)$$

However, the numerical treatment of the above minimization problem (11) is still infeasible, due to the presence of the high-dimensional integrals over  $\Omega \subset \mathbb{R}^d$ . To handle this problem we replace the exact integral by a numerical quadrature.

We compute the norm  $\|\cdot\|_V$  using Monte-Carlo integration, e.g.

$$v_{(U,N,M)}^\alpha = \arg \min_{v \in U} \mathcal{R}_{N,M}^\alpha(v, v),$$

$$\mathcal{R}_{N,M}^\alpha(v, v) = \frac{1}{N} \sum_{i=1}^N |v(x_i) - \frac{1}{M} \sum_{j=1}^M \int_0^{\eta \wedge \tau} r(x_i^{j,\alpha}(t)) dt + v(x_i^{j,\alpha}(\eta \wedge \tau))|^2, \quad (12)$$

where  $x_i^{j,\alpha}(0) = x_i$  for  $i = 1, \dots, N$ . We remark, that we have two Monte Carlo approximations: The first for integrating the stochastic differential equation (2) with different paths  $t \mapsto x_i^{j,\alpha}(t)$ ,  $j = 1, \dots, M$ . And the second Monte Carlo integration for different initial values  $x = x_i$ ,  $i = 1, \dots, N$  for setting up the Least Squares functional (11). The integral term  $\int_0^{\eta \wedge \tau} r(x_i^{j,\alpha}(t)) dt$  in (12) is then computed by a trapezoid rule. The different paths are computed by Euler Mayurana scheme [54] at discrete times  $t_k$  and the remaining integral in the formulars above are approximated by trapezoidal rule.

Let us highlight that the the input data are noisy due to stochastic nature of the SDE. Therefore, the Least Squares method is prone to over-fitting problems. Moreover, an accurate computation of the updated policy, and therefore an accurate approximation of the gradient of  $v^\alpha$  is ultimately important for the convergence of the Policy Iteration.

**Regularisation** To improve the accuracy, we can enforce better regularity of  $v$  by choosing an appropriate norm  $\|\cdot\|_F$ . In the numerical calculations, we add a regularization term, such that the actual risk functional is

$$\tilde{\mathcal{R}}_{N,M}^\alpha(v, v) := \mathcal{R}_{N,M}^\alpha(v, v) + \delta \|v\|_F^2.$$

By choosing  $\|\cdot\|_F$  as the  $\ell_2$  norm of the coefficient tensor  $A$  of  $v$  the regularization term depends on the choice of univariate basis functions. Presently, we used mixed (tensor product) Sobolev norms and refer to remark 2 for a brief discussion. To avoid deviation of the solution caused by the penalty term, we decrease the penalty parameter adaptively during the ALS iteration process in dependence of the current residual [55]. For any other iterative solver of (12) this procedure can be done analogously.

We have experienced that this part plays a crucial role for the performance of the algorithm. In our present examples, our method provided quite accurate results. However, for non-smooth viscosity solutions arising from more difficult problems we expect that improved techniques will be required.

The present optimization problem is tractable by local optimization methods on non-linear manifolds. Nevertheless, it remains hard to find an exact minimizer, see e.g. [56] for further discussion.

**Error Estimates** The theoretical justification of this Least Squares Monte Carlo approach is in a very early stage. Indeed, we are committing variational crimes, since we have replaced the original risk functional by an empirical risk functional. This introduces an additional error term, even if we assume that we have computed the exact minimizer of (14). For first theoretical results, we import well known results from *empirical risk minimization* in machine learning [57, 58]. Empirical risk minimisation has been considered for the regression problem in statistical learning theory. However, the present problem is not directly a regression problem, but the theory [57] can be straightforwardly extended to the present optimization problem, which we called *Variational Monte Carlo*. This term has been invented in physics earlier, but Monte Carlo Least Squares method seems be also an appropriate name. The error  $\mathcal{E} = \|v^\alpha - v_{(U,N,M)}^\alpha\|_v^2$  is split into three parts

$$\mathcal{E} = \mathcal{E}_{\text{approximation}} + \mathcal{E}_{\text{generalization}} + \mathcal{E}_{\text{optimization}}.$$

Due to the uncertain nature of the problem, we cannot expect to show convergence for the generalization term. Instead, we consider convergence in probability. In particular, the probability that a given error estimates fails, i.e.  $\mathbb{P}[\mathcal{E}_{\text{generalisation}} > \varepsilon]$ , decays exponentially with the number of sample points.

As a first result we recall to following corollary. Under certain assumption, one can show that

$$\mathbb{P}[\|v^\alpha - v_{(U,M,N)}^\alpha\|_{L^2(\Omega)}^2 > \varepsilon] \leq c_1(\varepsilon, U)e^{-c_2 N \varepsilon^2}$$

with  $c_1(\varepsilon, U), c_2 > 0$ .

See e.g Theorem 4.12, Corollary 4.19 and Corollary 4.22 from [59].

Overfitting effects introduced by the above interpolation procedure spoil the computation of the optimal policy  $\alpha$  more dramatically, since this requires the gradient of  $v^\alpha$  (14). We have experienced this effect in our computation. For a theoretical justification, it would be desirable that the error can be estimated in much stronger norms, e.g w.r.t. Lipschitz-norms etc.. In the result mentioned above, it was only measured w.r.t an  $L_2$ -norm.

**A Regression Problem** Let us highlight, that the present approach is NOT *learning*. It is NOT a statistical task, but a numerical method to solve an operator equation. Instead of solving (12) directly, we use a fixed point iteration

$$v_{k+1} := \arg \min_{v \in U} \mathcal{R}_{N,M}^\alpha(v, v_k).$$

In fact, this constitutes a regression problem.

## 5 Tree Based Tensor Representation - Tensor Trains

For large dimensions  $n$ , traditional ansatz functions, e.g. finite elements, splines, multi-variate polynomials etc. are not appropriate for the numerical solution of the PDE, since they are facing the curse of dimensions.

To this end we choose an underlying finite dimensional but large subspace  $V_p \subset V = L^2(\Omega)$  for the approximation of the sought value function.

First we choose a suitable approximation space for univariate approximation of functions  $x_i \mapsto f(x_i)$ ,  $i = 1, \dots, n$ . Presently, we have taken one-dimensional polynomials  $\phi_i = \text{span}\{\phi_{i_l} | 0 \leq i_l \leq p_i\}$  of degree  $p_i$ . However, other choices like splines waveletes etc. are also possible.

For the  $n$ -variate case, we consider the tensor product of such polynomial spaces

$$V_p := \text{span} \{ \phi_1 \otimes \dots \otimes \phi_n : \text{deg} \phi_i \leq p_i \}.$$

This is a space of multivariate (tensor product) polynomials with bounded multi-degree  $\mathbf{p} = (p_1, \dots, p_n)$ . For the sake of simplicity we have chosen the same degree in all coordinates, i.e.  $p_i = p$ ,  $i = 1, \dots, n$ .

A function  $q \in V_p$  can be expanded w.r.t. to tensor product basis functions via

$$q(x_1, \dots, x_n) = \sum_{i_1, \dots, i_n=1}^{p_1, \dots, p_n} A(i_1, \dots, i_n) \phi_{i_1}(x_1) \dots \phi_{i_n}(x_n).$$

Interpreting the coefficient representation  $(i_1, \dots, i_n) \mapsto A(i_1, \dots, i_n)$  of a polynomial  $q$  in this vector space as a tensor of order  $n$ , we need storage in  $\mathcal{O}(p^n)$  for the coefficient tensor  $A \in \otimes_{j=1}^n \mathbb{R}^p$ .

Let us note that  $\bigcup_{p \in \mathbb{N}} V_p$  is dense in  $V$ . Although the dimension of  $V_p$  is finite

$$\dim V_p = (p+1)^n$$

it is prohibitively large.

In the ambient space  $V_p$ , we consider a non-linear, possibly low-dimensional manifold, given by *tree based tensor representations* (hierarchical (Tucker) tensors - HT tensors) [60]. In the present applications, we choose so-called tensor trains (TT tensors), invented by Oseledets in [61, 62], which has considerably smaller dimensions [63]. They have been applied to various high-dimensional PDE's [64], but the parametrization has been used in quantum physics much earlier as *Matrix Product States* and *Tensor Network States*, successfully for the approximation of spin systems and Hubbard models. For a good survey we refer to the papers [56, 65–67]. The tensor train representation have appealing properties making them attractive for treatment of the present problems, compare [20]. For example they contain sparse polynomials, but are much more flexible

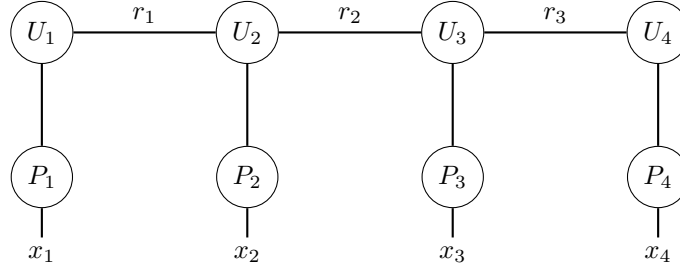


**Figure 2:** Graphical representation of TT tensor train induced polynomial in four variables.

at a price of a slightly larger overhead, see e.g. [68] for a comparison concerning parametric PDEs. Let us give brief introduction for a first understanding.

In order to get some notion of the representation and compression, we introduce the TT-rank  $\mathbf{r} \in \mathbb{N}^{n-1}$  of the tensor  $A \in \mathbb{R}^{(p_1, \dots, p_{n-1})}$  as element-wise smallest tuple such that

$$A(i_1, \dots, i_n) = \sum_{k_1, \dots, k_{n-1}=1}^{r_1, \dots, r_{n-1}} U_1(i_1, k_1) \cdot U_2(k_1, i_2, k_2) \cdots U_n(k_{n-1}, i_n)$$

holds for some  $U_i \in \mathbb{R}^{r_{i-1} \times p_i \times r_i}$  for  $i = 1, \dots, n$ . The TT-rank is well defined and the set of tensors of fixed TT-rank  $\mathbf{r}$  forms a smooth manifold of dimension in  $\mathcal{O}(npr^2)$  [63] in contrast to  $\mathcal{O}(n^p)$  of the ambient linear space  $V_p$ . Taking the closure of this set, see e.g. [60] we allow also tensors with smaller TT-rank denoted by  $\mathcal{M} := \mathcal{M}_{\leq \mathbf{r}}$  [56]. This slightly larger set forms an *algebraic variety* [56, 69]. However, numerical routines like ALS [55] do not differentiate between the variety and the manifold. For a survey and mathematical theory we refer to the literature, e.g. [56, 60, 67].

TT tensors can represent polynomials as follows. Let us consider the vectors

$$P_i : \mathbb{R} \rightarrow \mathbb{R}^{p_i+1} \text{ with } P_i(x) = \begin{bmatrix} 1 \\ \phi_0(x) \\ \phi_1(x) \\ \vdots \\ \phi_{p_i}(x) \end{bmatrix} = \begin{bmatrix} 1 \\ x \\ x^2 \\ \vdots \\ x^{p_i} \end{bmatrix}.$$

Then

$$\begin{aligned} p(x_1, \dots, x_n) &= \sum_{i_1, \dots, i_n}^{p_1, \dots, p_n} \sum_{k_1, \dots, k_{n-1}}^{r_1, \dots, r_{n-1}} U_1(i_1, k_1) U_2(k_1, i_2, k_2) \cdots U_n(k_{n-1}, i_n) (P_1(x_1))_{i_1} (P_2(x_2))_{i_2} \cdots (P_n(x_n))_{i_n} \\ &= \sum_{i_1, \dots, i_n}^{p_1, \dots, p_n} \sum_{k_1, \dots, k_{n-1}}^{r_1, \dots, r_{n-1}} U_1(i_1, k_1) U_2(k_1, i_2, k_2) \cdots U_n(k_{n-1}, i_n) \phi_{i_1}(x_1) \phi_{i_2}(x_2) \cdots \phi_{i_n}(x_n) \end{aligned}$$

is a multivariate polynomial of degree  $(\sum_i p_i)$ .

Using the graphical tensor network representation [56, 66] this polynomial can be interpreted as in Figure 2.

**Remark 2.** Note that other polynomial basis functions can be chosen as well. For numerical reasons we choose a set of orthogonal polynomials, e.g.  $\phi_i = \ell_i$  Legendre polynomials. In this case, Parseval formula provides a norm equivalence between  $L_2$  and  $\ell_2$ , which guarantees stability of our representations and approximation schemes. Presently, we have chosen one-dimensional  $H^1(I)$  orthogonal polynomials. The stability is enforced by an additional regularization term, and the penalty parameter has been adaptively reduced through the iteration procedures. This procedure enforces the approximations to have small  $L_\infty$  and even Lipschitz bounds.

In general, the set of one-dimensional basis functions can be modified to fit better to other norms rather than  $L_2$  or  $H_1$ .

It turns out, that optimization procedures in this TT format can be solved by consecutively optimizing one component  $U_i$  while the others are fixed. This alternating Least-Squares (ALS) algorithm converges to a local minimum [55]. Further details on the implementation in a similar context can be found in [21].

**Remark 3.** The present tensor ansatz has been proved by our experience to provide an advantageous choice, however there are some alternatives, well known in machine learning which can be used for the present purpose in same fashion or with some more or less obvious modifications. Among them are sparse grids [70], sparse polynomials [71], kernel methods (SVM) [72], in particular with polynomial kernels, and deep neural networks (DNN) [73].

In this respect, the essence of the present paper is not restricted to tree based tensor methods.

## 6 Formal Scaling with Respect to the Spatial Dimensions

We add a brief discussion about the computational complexity, and how the computational complexity scale with the spatial dimensions  $n$ , and how the HJB is prone to the curse of dimension.

Let us assume that we want to achieve a fixed accuracy  $\epsilon$ , i.e. we do not consider the scenario  $\epsilon \rightarrow 0$ . This is motivated because we want to keep the feedback law fairly simple, since this is required for an online feedback law.

The number of degrees of freedom of the underlying TT tensor is  $K \leq n(p+1)r^2 = \mathcal{O}(n)$  for fixed accuracy. Note that  $p = p(\epsilon)$ , and  $r = r(\epsilon)$  and will kept as constants in the sequel. (Presently  $p = 10, n = 6, r = 5$ .) In this regime  $K \sim n$  scales linearly with  $n$  instead of exponentially. This linear scaling behavior for storing the value function, seems to be quite optimal. We have rendered the curse of dimensions in a perfect way.

We further assume that we need at least  $N = \mathcal{O}(K)$  sample points, which is very optimistic. This is the best scaling we can expect, and extremely optimistic, and cannot be improved by other methods like kernel methods or DNN. The best proven rate for linear Least Squares methods is  $N \sim K \log K$  [74], and we neglect further logarithmic terms. Therefore the total numerical Work scales at least  $\mathcal{O}(nN) = \mathcal{O}(n^2)$ . With the present approach we have to calculate at each sample points  $M$  paths. Then, the total numerical work is  $\mathcal{O}(n^2MS)$ , where  $S$  is the work for computing a single path.

For linear function  $f$  fully connected, i.e. it is represented by fully populated matrix, the minimal cost for each path is  $S = \mathcal{O}(n^2T)$ , where  $T$  is the number of time steps. In this case we have assumed that the evaluation of the feedback law which scales with  $0 = (n^2m)$ , where  $m$  is the number of controls. When  $n \sim m$  the we can have an additional factor  $n$ , in the scaling of  $S$ . This does not happen in present case. We summarize that the total work is

$$\mathcal{O}(n^4p^2r^4MT) \text{ or for fixed accuracy } \mathcal{O}(n^4).$$

In the deterministic case we save the factor  $M$ , since we need only a single trajectory for each sample  $x^i$ . i.e. for each initial condition. Let us remark, if we use the (linearized) HJB directly, in a Least Squares setting, the factor  $MT$  is no longer apparent. We save also an additional factor  $n$ . Here, the scaling will be  $\mathcal{O}(n^3p^2r^4)$ . Indeed, this can save computing time at a price of less stability and a loss of accuracy. We will discuss this issue in the outlook.

In the subsequent numerical tests, we had around  $K = 800$  DOF in our models set. We took  $N = 10K \approx 8.000$  sampled initial values. For each initial value  $x_i$  we consider 100 paths, i.e. in each iteration step we performed  $8 \cdot 10^5$  runs of the Euler Mayurama scheme with 100 time steps. This part was by far the most time consuming part. However it can be perfectly parallelized, which has not been done so far.

The above scaling is estimated in a very optimistic fashion, and can be considered more as a lower bound. However, there are situations where the scaling is better, e.g. the matrix representation of  $f$  is sparse. It may be that multi-level Monte Carlo can provide an additional better scaling. All possibilities to reduce the present scaling  $\mathcal{O}(n^4)$  have to be considered in next future.

For other model sets, known in machine learning, the scaling can be worse. For a fully connected DNN with  $\mathcal{O}(n)$  neurons in each layer, and fixed depth  $L$  we have  $K = \mathcal{O}(Ln^2)$  DOFs, and assuming  $N \sim K$  like in the above setting, we obtain the scaling  $\mathcal{O}(n^4 L^2 n^2 MT) = \mathcal{O}(n^6)!$  For kernel methods  $\mathcal{O}(N^3 n^2 MT)$ , where the scaling w.r.t to the dimension  $n$  number of samples  $N = N_K$  is not clear. Assuming  $N \sim N$  seems to be quite optimistic.

## 7 Numerical Results

We present results of numerical tests for different optimal control problems. For the implementation of the tensor networks we use the open source c++ library `xerus` [75]. We also make use the python packages `Numpy`[76, 77] and `scipy`[78]. The calculations were performed on a AMD Phenom II 4x 3.20GHz, 16 GB RAM Fedora 31 Linux distribution. In every test we consider a compact set  $E = \Xi^C$  where we want to steer the state to and a cost functional of the form

$$\mathcal{J}(x_0, u) = \mathbb{E} \int_0^\tau 1 + \frac{1}{2}|u_t|^2 dt.$$

The equations are defined on a set  $\Omega$  and we denote by  $E = \Omega \setminus \Xi$  the set that we aim to steer the state to. The first two tests are simple one-dimensional problems, where the exact solution is known either analytically or numerically. The third test has a two-dimensional state space and finally we test the algorithm on a 6 dimensional state space.

**Remark 4.** In the following, we distinguish between the policy  $\alpha$ , the corresponding policy estimation function  $v$  and the policy evaluation function  $\mathcal{J}(\cdot, \alpha(\cdot))$ . For fixed  $x$ , we obtain  $v(x)$  by simply evaluating  $v$ . Here, no trajectory has to be computed. We obtain  $\mathcal{J}(x, \alpha(x))$  by numerically integrating along the trajectory with initial condition  $x$ . Note that  $\mathcal{J}(x, \alpha(x))$  is basically the numerical approximation of the cost functional with respect to a policy, defined in (3).

**Remark 5.** Within the test cases we specify the constants that we chose. Namely, the length of the trajectory  $\tau$ , the number of spacial samples  $N$ , the number of repetitions for every sample  $M$  and, as we set  $N$  proportional to the degrees of freedom of the tensor train representation of  $v$ , we also state the number of degrees of freedom. Note that for the numerical tests the length of the trajectory does not necessarily have to be the step-size of the Euler-Majurama scheme for solving the SDE. In fact, for every test we use a step size of 0.001 for the Euler-Majurama scheme. The length of the trajectory is mostly set to 0.1, which means that 100 steps within the SDE solver are used, c.f. [21, Section 6].

For every test we set the regularization constant  $\delta$  to be adaptive. In the beginning of every 'left-to-right sweep' within the ALS algorithm, we set  $\delta$  to be the current residuum  $\mathcal{R}_{N,M}^\alpha$ .

### 7.1 Test 1. One-dimensional exit time problem: Eikonal equation

We first test our algorithm with a simple one dimensional, deterministic problem, where the exact solution is known, namely the Eikonal equation on  $\Omega = [-2, 2]$ , i.e.

$$\dot{x} = u, \quad x(0) = x_0, \quad \Xi = [-2, 1], E = [1, 2].$$

Note that this problem fits into our setting by setting  $\sigma = 0$  and  $b = 0$ . Here, the value function has the form

$$v^*(x) = \sqrt{2}(1 - x), \quad x < 1.$$

Indeed, by choosing a polynomial of degree 1 as ansatz space, the number of samples  $N = 2$  and the number of repeated samples  $M = 1$ , we are able to recover the value function nearly exactly, as seen in Figure 3. The length of the trajectory is set to  $\tau = 0.001$  Note that this example is particularly easy to calculate, because the optimal value function  $v^*$  on the domain  $(-\infty, 1)$  is already contained in the ansatz space, and we have set  $v(x) = 0$  on the exit set  $E$ . However, it is possible to extend the domain of the ODE to  $(-\infty, \infty)$  while maintaining  $E = [1, 2]$ . In this case, the corresponding HJB is the well known eikonal equation [42]

$$|v'(x)|^2 = 2$$

with boundary conditions  $v(1) = v(2) = 0$ . This Dirichlet problem has multiple weak solution, the mentioned value function  $v(x) = \max\{0, \sqrt{2}(|1.5 - x| - 0.5)\}$  is the unique viscosity solution [42, 79]. In this respect,

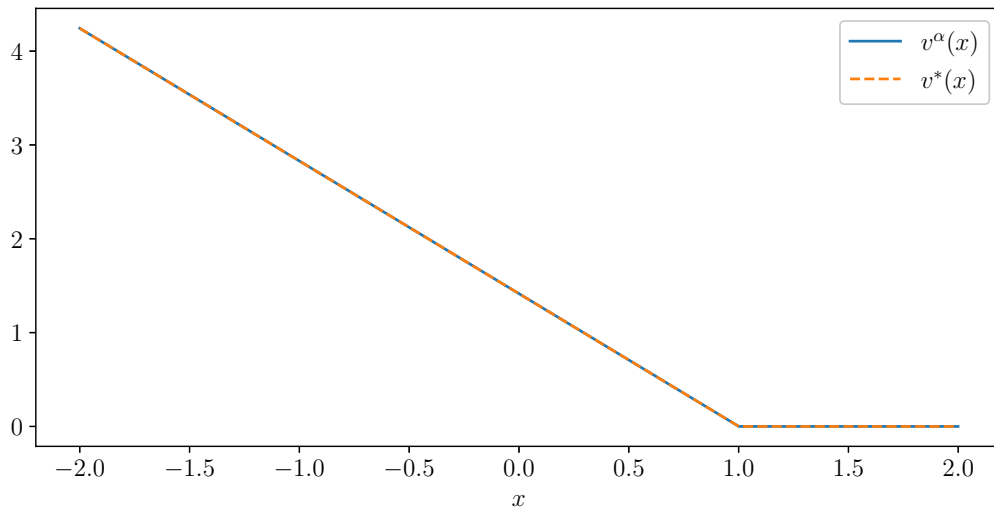


**Figure 3:** The value function  $v^*$  and the numerical approximation  $v^\alpha$ .

the present example is not so trivial and can be found in the literature for motivating the notion of viscosity solution. Let us remark, that the present value function  $v$  is still analytic in the exterior of the target set  $E = [1, 2]$ . As long as the abstract Policy Iteration (Algorithm 1) converges to a viscosity solution, we are going to approximate a viscosity solution. We refer to [80, 81] for a detailed discussion of this issue. We do not elaborate on this difficult issue and consider mainly classical solutions. Let us remark, that in the present example  $\sigma = 0$  and the dynamical system is deterministic.

We next analyze a more involved example, while still being in 1 dimension, namely the classical double well potential.

## 7.2 Test 2. One-dimensional double well potential

We next consider the double well potential on  $\Omega = [-2, 2]$  with  $\Xi = [-2, 1)$ ,  $E = [1, 2]$ .

$$pot(x) = 5(x^2 - 1)^2,$$

visualized in figure 4. The corresponding SDE is

$$dX_t = \nabla pot(X_t)dt + \sigma(X_t)dW_t + g(X_t)U_t(X_t)dt,$$

Here, we cannot expect the value function to be included in our ansatz space. Thus, we experiment with different polynomial degrees, visualized in figures 5a and 5b. For the computation of the controllers we set the number of samples to  $N = 10 \cdot dof$ , where  $dof$  is the polynomial degree increased by 1. We set the length of the trajectory to  $\tau = 0.1$  and compute for every sample  $M = 1000$  trajectories. Note that the length of the trajectory consists of 100 individual steps in the Euler-Majurana scheme, i.e.  $0.1 = 100 \cdot 0.001$ .

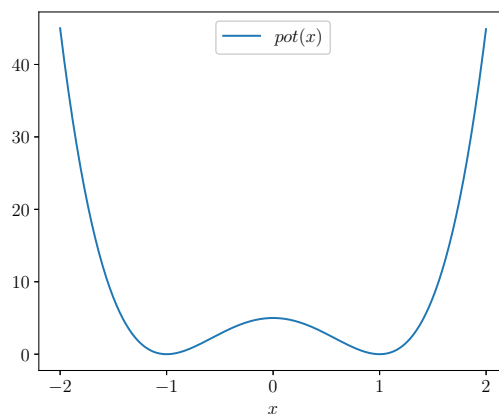
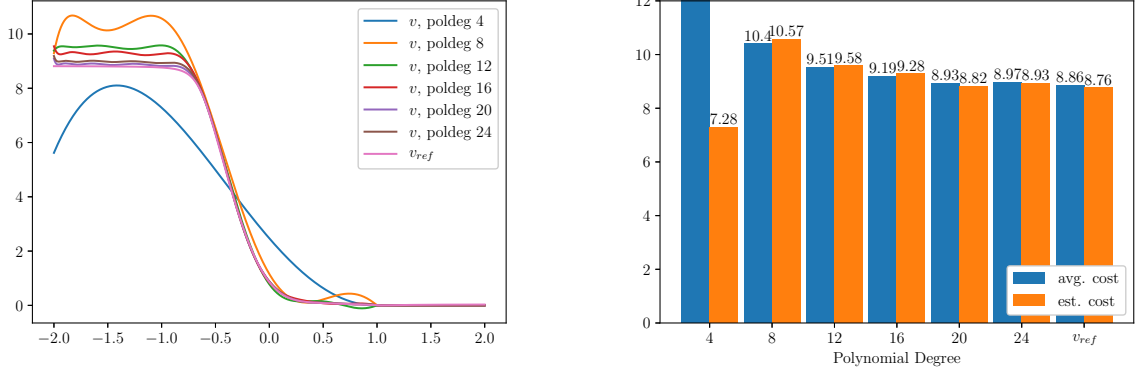


**Figure 4:** The double well potential  $pot$ .

We compare the results to a reference solution that is obtained by solving the HJB equation with a finite differences scheme with 3000 grid points.

We observe, that higher polynomial degrees yield a better approximation of the reference solution, with polynomial degree of 20 yielding the best results. We also deduce from figure 5a that we do not exactly

reproduce  $v_{ref}$ . From figure 5b we deduce that the performance of the controller of polynomial 20 is less than 1% higher than the performance of the reference solution.



(a) The approximated value functions and the reference solution. (b) Estimated cost and average cost by averaging over 10000 trajectories with initial value  $x_0 = -1$ . Avg. cost for polynomial degree 4 is 34.03.

**Figure 5:** One dimensional double well potential

### 7.3 Test 3. Two dimensional three-hole potential

We consider a two dimensional three-hole potential with one being less significant than the others. Note that this potential has already been used in different contexts and is sometimes referred to as Müller-Brown potential, see i.e. [82, 83]. In particular we have  $\Omega = [-3, 3]^2$  and

$$pot(x_1, x_2) = 3e^{-x_1^2 - (x_2 - 1/3)^2} - 3e^{-x_1^2 - (x_2 - 5/3)^2} - 5e^{-(x_1 - 1)^2 - x_2^2} - 5e^{-(x_1 + 1)^2 - x_2^2} + 0.2x_1^4 + 0.2(x_2 - 1/3)^4.$$

We choose a ball of radius 0.5 around  $x_{target} \approx [-1.048, -0.042]$  as target set  $E$  and set  $\Xi = \Omega \setminus E$ . Note that  $x_{target}$  contains a local minimum of  $pot$ . Both sets are visualized in figure 6a. Again, we compare the performance of controllers with different polynomial degree and see that higher order polynomials substantially increase the performance of the controllers. The best performance is achieved by a controller of polynomial degree 16. However, lower polynomial degree yields 'good' results as well. For the computation of the controllers we set the number of samples to  $N = 10 \cdot dof$ , where  $dof$  is again the number of degrees of freedom of the tensor train. In this two-dimensional example, we set the rank of the tensor train to be maximal for every polynomial degree. Further, we set  $M = 100$  and  $\tau = 0.1$ . In figure 7, we plot different trajectories of the dynamical system for both, the uncontrolled and controlled system. Note that the controlled trajectories get steered into the set  $E$  within the given time frame of 10, while the uncontrolled dynamics stay in the minimum on the right. Here, we visually see the effect of controlling this dynamical system. Figure 6b again visualizes the performance of controllers for different polynomial degrees.

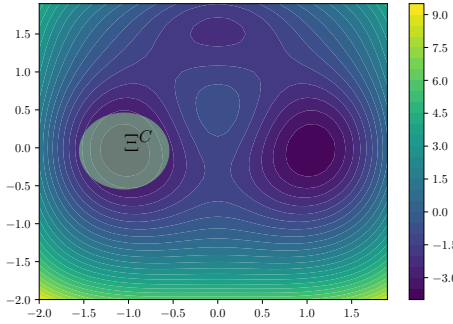
As the polynomial degree of 16 had the best performance, we add contour plots of the value function in Figure 8. In particular compare this Figure to those in [84], where a similar figure appears in a different context.

### 7.4 Test 4: Higher dimensional problem

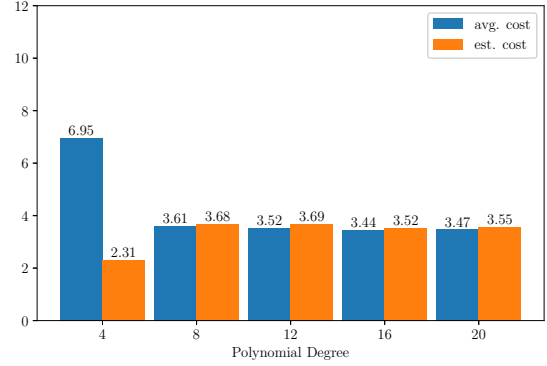
We consider the multi-dimensional Double Well potential

$$pot(x) = \sum_{i=1}^n \kappa_i (x_i^2 - 1)^2.$$

Note that this potential has  $2^n$  local minima and the choice of  $\kappa$  determines their metastability. In our test we use  $\kappa_i = 5$  for all  $i$ . The exit set  $E$  is  $B_{0.5\sqrt{n}}(1)$ , the ball of radius  $0.5\sqrt{n}$  around  $[1, \dots, 1] \in \mathbb{R}^n$ . We

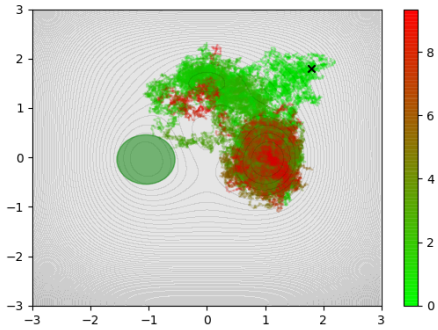


(a) The potential  $pot$  and the exit set  $\Xi^C$

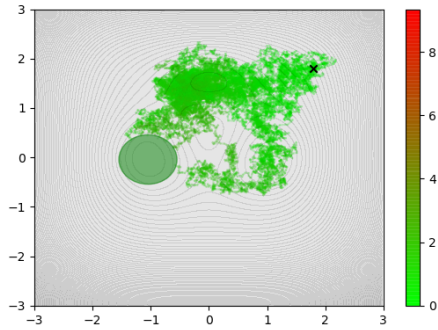


(b) Estimated cost and average cost by averaging over 10000 trajectories with initial value  $x_0 = [1.8, 1.8]$ .

**Figure 6:** Left: The potential  $pot$ . Right: Performance of controllers of different polynomial degree.



(a) Visualization of 10 trajectories, uncontrolled



(b) Visualization of 10 trajectories, controlled

**Figure 7:** Top: Plots of 10 trajectories, starting at  $x_0 = [1.8, 1.8]$ . The colors indicate the time within the trajectory, starting with green dots and ending with red dots. We stop the simulation at  $T = 10$  or when the exit set is reached. As no red dots appear for the controlled dynamics, we see that in this case the exit set is reached in a fast manner. The black cross is the initial value.

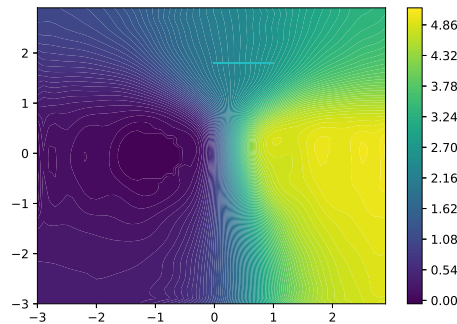
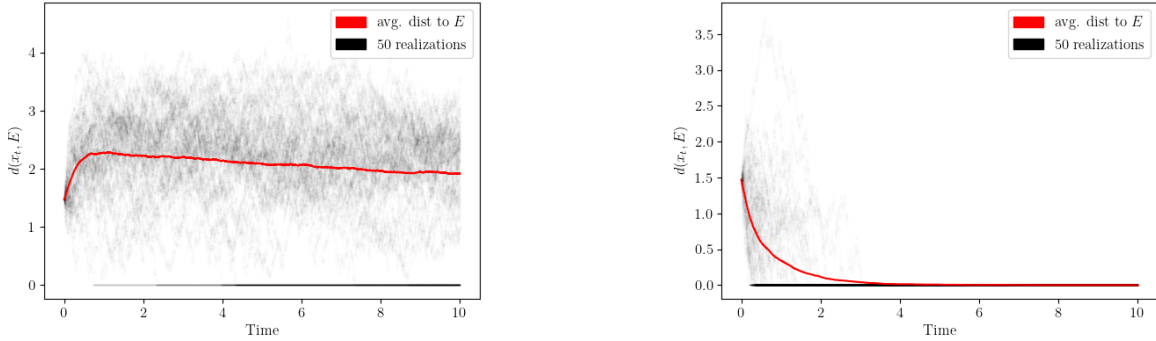


**Figure 8:** Contour plot of the approximation of the value function. Polynomial degree is 16.

further choose  $\Omega = [-\frac{\pi}{2}, \frac{\pi}{2}]^2$ . Note that while the radius of the exit set seems large, for the case  $n = 6$ , its volume is only 1.8% of the volume of  $\Omega$ . We further stress, that while in the dynamics the dimensions are independent from each other, we cannot expect the value function and thus also the policy to have a strict separation in the dimensions. Here, the curse of dimensions comes into play. Choosing a polynomial degree of 6 and a tensor train rank of  $[5, 5, 5, 5, 5]$  allows us to reduce the ansatz space from 46656 degrees of freedom to 770. Again, setting  $N = 10 \cdot dof$ ,  $M = 100$  and  $\tau = 0.1$  we visualize the resulting controller in figure 9. We start the trajectory at  $[-1, \dots -1] \in \mathbb{R}^n$ . We see that the uncontrolled dynamics approach the exit set slowly, while the controlled dynamics most trajectories have reached the exit set at time 3. The resulting cost of the controlled dynamics is 4.44 and the predicted cost 4.74. Note that computing the average cost for the uncontrolled dynamics is not feasible because of the high metastability of the minima, as seen in Figure 9.



(a) Red: average distance of the exit set to 1000 realizations of the uncontrolled dynamics. Black (dots): scatter plot of the distance of 50 realizations of the uncontrolled dynamics to the exit set.

(b) Red: average distance of the exit set to 1000 realizations of the controlled dynamics. Black (dots): scatter plot of the distance of 50 realizations of the controlled dynamics to the exit set.

**Figure 9:** Visualization of the distance of trajectories to the exit set.

## Conclusion and Outlook

We have considered a stochastic optimal control problem. In the SDE the control  $u$  enters as an affine function in  $u$  and in its corresponding cost functional  $\mathcal{J}$  quadratically. We solved this problem by using approximative Policy Iteration whereby we used dynamical programming with the linearized Bellman equation resulting in a linear operator equation (Koopman operator). The SDE was discretized by the Euler Mayurama method. The optimality condition has been derived from the HJB equation. For the numerical solution we employed tree based tensor approximations in the subspace of tensor product polynomials. For the computation of the Least Squares risk functional  $\mathcal{R}$  we used Monte Carlo integration. We have provided successful numerical test for moderate dimensions.

The Least-Squares method allows for incorporating additional penalty terms in (4, 12), which might be zero for the exact solution. Potential approaches include the following.

- The boundary condition  $v^\alpha = 0$  on  $\partial\Xi$ , by sampling the boundary and penalizing  $v^\alpha$  at these sample points.
- Incorporating the linearized HJB, cf. appendix A and (15) in the risk functional

The most time consuming step is the generation of many different paths (trajectories) that are the numerical solution of the SDE. The above penalty terms yield extra information about the system with low additional computational cost. In the next future we want to pursue this direction.

## References

- [1] W. H. Fleming. “Controlled Markov processes and mathematical finance”. In: *Nonlinear Analysis, Differential Equations and Control*. Ed. by F. H. Clarke, R. J. Stern, and G. Sabidussi. Dordrecht: Springer Netherlands, 1999, pp. 407–446.
- [2] Y. Peng and J. Li. *Stochastic Optimal Control of Structures*. Springer, 2019.
- [3] C. Schütte, S. Winkelmann, and C. Hartmann. “Optimal control of molecular dynamics using Markov state models”. In: *Math. Program. (Series B)* 134.1 (2012), pp. 259–282.
- [4] C. Hartmann, L. Richter, C. Schütte, and W. Zhang. “Variational characterization of free energy: theory and algorithms”. In: *Entropy* 19.11 (2017).
- [5] C. Hartmann, O. Kebiri, L. Neureither, and L. Richter. “Variational approach to rare event simulation using least-squares regression”. In: *Chaos: An Interdisciplinary Journal of Nonlinear Science* 29.6 (2019), p. 063107.
- [6] A. Kröner, A. Picarelli, and H. Zidani. “Infinite Horizon Stochastic Optimal Control Problems with Running Maximum Cost”. In: *SIAM Journal on Control and Optimization* 56 (09/2017).
- [7] E. N. Barron. “The Bellman equation for control of the running max of a diffusion and applications to look-back options”. In: *Applicable Analysis* 48.1-4 (1993), pp. 205–222. eprint: <https://doi.org/10.1080/00036819308840158>.
- [8] T. Damm, H. Mena, and T. Stillfjord. “Numerical solution of the finite horizon stochastic linear quadratic control problem”. In: *Numerical Linear Algebra with Applications* 24.4 (2017). e2091 nla.2091, e2091. eprint: <https://onlinelibrary.wiley.com/doi/pdf/10.1002/nla.2091>.
- [9] C. Hartmann and C. Schütte. “Efficient rare event simulation by optimal nonequilibrium forcing”. In: *Journal of Statistical Mechanics: Theory and Experiment* 2012.11 (11/2012), P11004.
- [10] N. Nüsken and L. Richter. *Solving high-dimensional Hamilton-Jacobi-Bellman PDEs using neural networks: perspectives from the theory of controlled diffusions and measures on path space*. 2020. eprint: 2005.05409.
- [11] M. Jensen and I. Smears. “On the Convergence of Finite Element Methods for Hamilton–Jacobi–Bellman Equations”. In: *SIAM Journal on Numerical Analysis* 51.1 (2013), pp. 137–162. eprint: <https://doi.org/10.1137/110856198>.
- [12] F. Bonnans and H. Zidani. “Consistency of Generalized Finite Difference Schemes for the Stochastic HJB Equation”. In: *SIAM Journal on Numerical Analysis* 41(3) (2003), pp. 1008–1021.
- [13] F. Bonnans, E. Ottenwaelter, and H. Zidani. “A fast algorithm for the two dimensional HJB equation of stochastic control”. In: *ESAIM: Mathematical Modelling and Numerical Analysis* 38(4) (2004), pp. 723–735.
- [14] M. Falcone and R. Ferretti. *Semi-Lagrangian Approximation Schemes for Linear and Hamilton–Jacobi Equations*. Philadelphia, PA: Society for Industrial and Applied Mathematics, 2013. eprint: <https://epubs.siam.org/doi/pdf/10.1137/1.9781611973051>.
- [15] M. Falcone. “A numerical approach to the infinite horizon problem of deterministic control theory”. In: *Applied Mathematics and Optimization* 15.1 (01/1987), pp. 1–13.
- [16] K. Debrabant and E. Jakobsen. “Semi-Lagrangian schemes for linear and fully non-linear Hamilton-Jacobi-Bellman equations”. In: *Hyperbolic Problems: Theory, Numerics, Applications*. Springer, 03/2014, pp. 483–490.
- [17] D. Tonon, M. Aronna, and D. Kalise. *Optimal Control: Novel Directions and Applications*. Springer, 01/2017.

- [18] J. Garcke and A. Kröner. “Suboptimal Feedback Control of PDEs by Solving HJB Equations on Adaptive Sparse Grids”. In: *Journal of Scientific Computing* 70.1 (2017). also available as INS Preprint No. 1518, pp. 1–28.
- [19] O. Bokanowski, J. Garcke, M. Griebel, and I. Klompaker. “An Adaptive Sparse Grid Semi-Lagrangian Scheme for First Order Hamilton-Jacobi Bellman Equations”. English. In: *Journal of Scientific Computing* 55.3 (2013). also available as INS Preprint No. 1207, pp. 575–605.
- [20] S. Dolgov, D. Kalise, and K. Kunisch. “A Tensor Decomposition Approach for High-Dimensional Hamilton-Jacobi-Bellman Equations”. In: *arXiv e-prints*, arXiv:1908.01533 (08/2019), arXiv:1908.01533. arXiv: 1908.01533 [math.OC].
- [21] M. Oster, L. Sallandt, and R. Schneider. *Approximating the Stationary Hamilton-Jacobi-Bellman Equation by Hierarchical Tensor Products*. 2019. arXiv: 1911.00279 [math.OC].
- [22] M. Akian and E. Fodjo. “Probabilistic Max-Plus Schemes for Solving Hamilton-Jacobi-Bellman Equations”. In: *Numerical Methods for Optimal Control Problems*. Ed. by M. Falcone, R. Ferretti, L. Grüne, and W. M. McEneaney. Cham: Springer International Publishing, 2018, pp. 183–209.
- [23] B. Luo, H.-N. Wu, T. Huang, and D. Liu. “Data-based approximate policy iteration for affine nonlinear continuous-time optimal control design”. In: *Automatica* 50.12 (2014), pp. 3281–3290.
- [24] B. Kafash, A. Delavarkhalafi, and S. Karbassi. “Application of variational iteration method for Hamilton–Jacobi–Bellman equations”. In: *Applied Mathematical Modelling* 37.6 (2013), pp. 3917–3928.
- [25] J. Lawton and R. W. Beard. “Numerically efficient approximations to the Hamilton-Jacobi-Bellman equation”. In: *Proceedings of the 1998 American Control Conference. ACC (IEEE Cat. No.98CH36207)*. Vol. 1. 06/1998, 195–199 vol.1.
- [26] J. Han and W. E. “Deep Learning Approximation for Stochastic Control Problems”. In: *ArXiv abs/1611.07422* (2016).
- [27] J. Han, A. Jentzen, and W. E. “Solving high-dimensional partial differential equations using deep learning”. In: *Proceedings of the National Academy of Sciences* 115.34 (2018), pp. 8505–8510. eprint: <https://www.pnas.org/content/115/34/8505.full.pdf>.
- [28] H. Pham, X. Warin, and M. Germain. *Neural networks-based backward scheme for fully nonlinear PDEs*. 2020. arXiv: 1908.00412 [math.OC].
- [29] R. A. Howard. *Dynamic programming and Markov processes*. The Technology Press of the MIT. J. Wiley. Cambridge MA, New York, 1960.
- [30] R. Bellman. “Functional equations in the theory of dynamic programming— v : positivity and quasi-linearity”. In: *Proc Natl Acad Sci U S A* 41 (10/1955), pp. 743–746.
- [31] R. Bellman. *Dynamic Programming*. Princeton University Press, Princeton, 1961.
- [32] M. Nisio. *Stochastic Control Theory. Dynamic Programming Principle*. 2nd ed. Springer Japan, 2015. eprint: 978-4-431-55123-2.
- [33] G. Da Prato and J. Zabczyk. *Stochastic Equations in Infinite Dimensions*. Encyclopedia of Mathematics and its Applications. Cambridge University Press, 1992.
- [34] W. H. Fleming and H. Soner. *Control Markov Processes and Viscosity Solutions*. 2nd ed. Springer, 2006.
- [35] G. Fabbri, F. Gozzi, and A. Swiech. *Stochastic Optimal Control in Infinite Dimension*. Vol. 82. Springer, 01/2017.

- [36] C. Beck, S. Becker, P. Grohs, N. Jaafari, and A. Jentzen. *Solving stochastic differential equations and Kolmogorov equations by means of deep learning*. 2018. arXiv: 1806.00421 [math.NA].
- [37] J.-M. Bismut. “An Introductory Approach to Duality in Optimal Stochastic Control”. In: *SIAM Review* 20.1 (01/1978), pp. 62–78.
- [38] W. Fleming and H. Soner. *Control Markov Processes and Viscosity Solutions*. 2nd ed. Springer Science+Business Media, 2006.
- [39] L. Arnold. *Random Dynamical Systems*. eng. 1998.
- [40] L. Arnold and M. Scheutzow. “Perfect cocycles through stochastic differential equations”. In: *Probability Theory and Related Fields* 101 (1995), pp. 65–88.
- [41] B. Øksendal. *Stochastic Differential Equations: An Introduction with Applications*. Vol. 82. 01/2000.
- [42] M. Bardi and I. Capuzzo-Dolcetta. *Optimal Control and Viscosity Solutions of Hamilton-Jacobi-Bellman Equations*. Boston: Birkäuser, 01/1997.
- [43] R. Buckdahn and T. Nie. “Generalized Hamilton–Jacobi–Bellman Equations with Dirichlet Boundary Condition and Stochastic Exit Time Optimal Control Problem”. In: *SIAM Journal on Control and Optimization* 54.2 (01/2016), pp. 602–631.
- [44] D. Bertsekas. *Dynamic Programming and Optimal Control*. Volume 2, 4th Edition. Athena Scientific, 2019.
- [45] B. O. Koopman. “Hamiltonian Systems and Transformation in Hilbert Space”. In: *Proc. of the National Academy of Sciences* 17.5 (1931), pp. 315–318. eprint: <https://www.pnas.org/content/17/5/315.full.pdf>.
- [46] M. Dellnitz, G. Froyland, and S. Sertl. “On the isolated spectrum of the Perron-Frobenius operator”. In: *Nonlinearity* 13.4 (05/2000), pp. 1171–1188.
- [47] M. Dellnitz and O. Junge. “On the Approximation of Complicated Dynamical Behavior”. In: *SIAM Journal on Numerical Analysis* 36.2 (1999), pp. 491–515. eprint: <https://doi.org/10.1137/S0036142996313002>.
- [48] C. Schütte, A. Fischer, W. Huisinga, and P. Deuffhard. “A Direct Approach to Conformational Dynamics Based on Hybrid Monte Carlo”. In: *Journal of Computational Physics* 151.1 (1999), pp. 146–168.
- [49] A. Mauroy, I. Mezić, and Y. Susuki. *The Koopman Operator in System and Control*. Springer, 2019.
- [50] S. Klus, P. Koltai, and C. Schütte. “On the numerical approximation of the Perron-Frobenius and Koopman operator”. In: *J. of Computational Dynamics* 3.2158-2491-2016-1-51 (2016), p. 51.
- [51] A. Lasota. *Chaos, fractals, and noise : stochastic aspects of dynamics*. eng. 2. ed. Applied mathematical sciences BV000005274 97. Springer, 1994.
- [52] M. Budišić, R. Mohr, and I. Mezić. “Applied Koopmanism”. In: *Chaos: An Interdisciplinary J. of Nonlinear Science* 22.4 (2012), p. 047510.
- [53] N. Črnjarić-Žic, S. Maćešić, and I. Mezić. “Koopman Operator Spectrum for Random Dynamical Systems”. In: *arXiv e-prints*, arXiv:1711.03146 (11/2017), arXiv:1711.03146. arXiv: 1711.03146 [math.DS].
- [54] P. Kloeden and E. Platen. *Numerical Solution of Stochastic Differential Equations*. Springer, 1992.
- [55] S. Holtz, T. Rohwedder, and R. Schneider. “The Alternating Linear Scheme for Tensor Optimization in the Tensor Train Format”. In: *SIAM J. Sci. Comput.* 34.2 (2012), A683–A713. eprint: <https://doi.org/10.1137/100818893>.
- [56] M. Bachmayr, R. Schneider, and A. Uschmajew. “Tensor Networks and Hierarchical Tensors for the Solution of High-Dimensional Partial Differential Equations”. In: *Found. Comput. Math.* 16.6 (12/2016), pp. 1423–1472.
- [57] F. Cucker and S. Smale. “On the Mathematical Foundations of Learning”. In: *BULLETIN* 39 (11/2001).

- [58] I. Steinwart and A. Christmann. *Support Vector Machines*. 1st. Springer Publishing Company, Incorporated, 2008.
- [59] M. Eigel, R. Schneider, P. Trunschke, and S. Wolf. “Variational Monte Carlo—bridging concepts of machine learning and high-dimensional partial differential equations”. In: *Advances in Computational Mathematics* (10/2019).
- [60] W. Hackbusch. *Tensor Spaces and Numerical Tensor Calculus*. Vol. 42. Springer, 01/2012.
- [61] I. Oseledets and E. Tyrtyshnikov. “Breaking the Curse of Dimensionality, Or How to Use SVD in Many Dimensions”. In: *SIAM J. Sci. Comput.* 31 (01/2009), pp. 3744–3759.
- [62] I. Oseledets. “Tensor-Train Decomposition”. In: *SIAM J. Sci. Comput.* 33 (01/2011), pp. 2295–2317.
- [63] S. Holtz, T. Rohwedder, and R. Schneider. “On manifolds of tensors of fixed TT-rank”. In: *Numerische Mathematik* 120.4 (04/2012), pp. 701–731.
- [64] B. N. Khoromskij. “Tensors-structured numerical methods in scientific computing : survey on recent advances”. In: *Chemometrics and intelligent laboratory systems* 110.1 (2011), pp. 1–19.
- [65] W. Hackbusch and R. Schneider. *Tensor Spaces and Hierarchical Tensor Representations*. Cham: Springer International Publishing, 2014, pp. 237–261.
- [66] S. Szalay, M. Pfeffer, V. Murg, G. Barcza, F. Verstraete, R. Schneider, and Ö. Legeza. “Tensor product methods and entanglement optimization for ab initio quantum chemistry”. In: *International j. of quantum chemistry* 115.19 (2015), pp. 1342–1391.
- [67] W. Hackbusch. “Numerical tensor calculus”. In: *Acta numerica* 23 (2014), pp. 651–742.
- [68] M. Bachmayr, A. Cohen, and W. Dahmen. “Parametric PDEs: sparse or low-rank approximations?”. In: *IMA J. of Numerical Analysis* 38.4 (09/2017), pp. 1661–1708. eprint: <http://oup.prod.sis.lan/imagna/article-pdf/38/4/1661/25956676/drx052.pdf>.
- [69] B. Kutschan. “Tangent cones to tensor train varieties”. In: *Linear Algebra and its Applications* 544 (2018), pp. 370–390.
- [70] H.-J. Bungartz and M. Griebel. “Sparse grids”. In: *Acta Numerica* 13 (2004), pp. 147–269.
- [71] M. Bachmayr, A. Cohen, D. Dung, and C. Schwab. “Fully Discrete Approximation of Parametric and Stochastic Elliptic PDEs”. In: *SIAM J. Numer. Anal.* 55.5 (2017), pp. 2151–2186.
- [72] B. Scholkopf and A. J. Smola. *Learning with Kernels: Support Vector Machines, Regularization, Optimization, and Beyond*. Cambridge, MA, USA: MIT Press, 2001.
- [73] I. Goodfellow, Y. Bengio, and A. Courville. *Deep Learning*. <http://www.deeplearningbook.org>. MIT Press, 2016.
- [74] A. Cohen and G. Migliorati. “Optimal weighted least-squares methods”. working paper or preprint. 08/2016.
- [75] B. Huber and S. Wolf. *Xerus - A General Purpose Tensor Library*. <https://libxerus.org/>. 2014–2017.
- [76] S. Van Der Walt, S. C. Colbert, and G. Varoquaux. “The NumPy array: a structure for efficient numerical computation”. In: *Computing in Science & Engineering* 13.2 (2011), p. 22.
- [77] T. E. Oliphant. *A guide to NumPy*. Vol. 1. Trelgol Publishing USA, 2006.
- [78] P. Virtanen, R. Gommers, T. E. Oliphant, M. Haberland, T. Reddy, D. Cournapeau, E. Burovski, P. Peterson, W. Weckesser, J. Bright, S. J. van der Walt, M. Brett, J. Wilson, K. Jarrod Millman, N. Mayorov, A. R. J. Nelson, E. Jones, R. Kern, E. Larson, C. Carey, Í. Polat, Y. Feng, E. W. Moore, J. Vand erPlas, D. Laxalde, J. Perktold, R. Cimrman, I. Henriksen, E. A. Quintero, C. R. Harris, A. M. Archibald, A. H. Ribeiro, F. Pedregosa, P. van Mulbregt, and S. 1. 0. Contributors. “SciPy 1.0: Fundamental Algorithms for Scientific Computing in Python”. In: *Nature Methods* 17 (2020), pp. 261–272.
- [79] M. G. Crandall and P.-L. Lions. “Viscosity solutions of Hamilton-Jacobi equations”. In: *Transactions of the American mathematical society* 277.1 (1983), pp. 1–42.

- [80] S. D. Jacka and A. Mijatović. “On the policy improvement algorithm in continuous time”. In: *Stochastics* 89.1 (2017), pp. 348–359. eprint: <https://doi.org/10.1080/17442508.2016.1187609>.
- [81] B. Kerimkulov, D. Šiška, and L. Szpruch. “Exponential Convergence and Stability of Howard’s Policy Improvement Algorithm for Controlled Diffusions”. In: *SIAM Journal on Control and Optimization* 58.3 (2020), pp. 1314–1340. eprint: <https://doi.org/10.1137/19M1236758>.
- [82] S. Huo and J. E. Straub. “The MaxFlux algorithm for calculating variationally optimized reaction paths for conformational transitions in many body systems at finite temperature”. In: *The Journal of Chemical Physics* 107.13 (10/1997), pp. 5000–5006.
- [83] S. Park, M. K. Sener, D. Lu, and K. Schulten. “Reaction paths based on mean first-passage times”. In: *The Journal of Chemical Physics* 119.3 (07/2003), pp. 1313–1319.
- [84] C. Hartmann, R. Banisch, M. Sarich, T. Badowski, and C. Schütte. “Characterization of Rare Events in Molecular Dynamics”. In: *Entropy* 16.1 (12/2013), pp. 350–376.
- [85] S. Peng. “A Generalized dynamic programming principle and hamilton-jacobi-bellman equation”. In: *Stochastics and Stochastic Reports* 38.2 (1992), pp. 119–134. eprint: <https://doi.org/10.1080/17442509208833749>.
- [86] G. A. Pavliotis. *Stochastic processes and applications: diffusion processes, the Fokker-Planck and Langevin equations*. Vol. 60. Springer, 2014.

## A Alternate approach via solving the HJB

In this section we consider an alternative approach to finding the value function. Indeed, instead of considering the Bellman equation, one can instead consider the Hamilton-Jacobi-Bellman (HJB) equation. It has the form [43, 85]

$$\begin{aligned} \sigma^2(x)\Delta v^*(x) + \min_{\alpha \in F} \{ \nabla v^*(x) \cdot (b(x) + g(x)\alpha(x)) + r(x, \alpha(x)) \} &= 0 \text{ on } \Xi \\ v^* &= 0 \text{ on } \partial\Xi \end{aligned} \quad (13)$$

with a Dirichlet boundary condition. For the exact value function, and the present reward  $r^\alpha(x) = c(x) + \alpha(x)^T B \alpha(x)$ , the minimization within (13) w.r.t. the parameter  $\alpha$  can be carried out explicitly. This yields optimality condition for the optimal policy (feedback law) given by [42]

$$\alpha^*(x) = -\frac{1}{2} B^{-1} g(x)^T \nabla v^*(x). \quad (14)$$

Denoting  $f^\alpha(x) := b(x) + g(x)\alpha(x)$  and  $r^\alpha(x) = r(x, \alpha(x))$  and  $r_t^\alpha(x) := r^\alpha(\Phi_t^\alpha(x))$  the corresponding HJB in coupled form is

$$\begin{aligned} 0 &= \sigma^2(x)\Delta v^*(x) + \nabla v^*(x) \cdot f^{\alpha^*}(x) + r^{\alpha^*}(x) \\ \alpha^*(x) &= -\frac{1}{2} B^{-1} g(x)^T \nabla v^*(x). \end{aligned}$$

Similar to the approach in Section 2 for given  $\alpha$  we have the linear PDE

$$0 = \sigma^2 \Delta v^\alpha + \nabla v^\alpha \cdot f^\alpha + r^\alpha \quad (15)$$

to compute the policy evaluation function  $v^\alpha$ . Note that this equation corresponds to (6) in the Bellman setting.

As the Policy Iteration algorithm is based on computing  $v^\alpha$ , one can exchange (8) with (15) within the Policy Iteration algorithm. This linearized HJB equation is a stationary inhomogenous backward Kolmogorov equation and thus a deterministic linear PDE in a possibly high-dimensional space. The stochastic nature of the underlying dynamical system is expressed in the additional viscosity term, i.e. Laplacian  $\Delta$ . Indeed, the computational bottleneck is the numerical solution of this high dimensional PDE. Note that the direct connection between the Koopman operator corresponding to the linearized Bellman equation and the linearized HJB equation is that the backward Kolmogorov operator is the generator of the Koopman operator semi-group, see i.e. [86].

## B Reinterpretation of the finite exit time problem as an infinite horizon problem

In this section we give an informal way to interpret the finite exit time problem as an non smooth infinite horizon optimal control problem. Taking this viewpoint has the advantage that standard HJB theory can be (formally) applied and that the usual Koopman operator without the stop time  $\eta$  can be defined. Note that our implementation we use this viewpoint. To this end we restate the finite exit time problem

$$\mathcal{J}(x, u) = \mathbb{E} \int_0^\eta c(X_t) + u_t^T B u_t dt,$$

subject to

$$\begin{aligned} dX_t &= b(X_t)dt + \sigma(X_t)dW_t + g(X_t)u_t dt \\ X_0 &= x \end{aligned}$$

and

$$\eta = \inf\{t > 0 | X_t \notin \Xi\}.$$

Denoting the characteristic function on  $\Xi$  by  $\chi_\Xi$  we can represent this problem as an infinite horizon problem in the following way.

$$\mathcal{J}(x, u) = \mathbb{E} \int_0^\infty \chi_\Xi(X_t)(c(X_t) + u_t^T B u_t) dt,$$

subject to

$$\begin{aligned} dX_t &= \chi_\Xi(X_t)(b(X_t)dt + \sigma(X_t)dW_t + g(X_t)u_t dt) \\ X_0 &= x. \end{aligned}$$

Note that the characteristic function basically sets the running cost and the dynamics to zero once the state is steered out of  $\Xi$ . Moreover, the dynamics and the cost functional is then non smooth.